Modification of the Proteolytic Fragmentation Pattern upon Oxidation of Cysteines from Ribulose 1,5-Bisphosphate Carboxylase/Oxygenase†

Julia Marín-Navarro and Joaquín Moreno*

Departament de Bioquímica i Biologia Molecular, Facultat de Biologia, Universitat de València Av. Dr. Moliner 50, Burjassot, València E-46100, Spain

Received September 23, 2003; Revised Manuscript Received October 15, 2003

ABSTRACT: The proteolytic susceptibility of the native CO_2-fixing photosynthetic enzyme ribulose 1,5-bisphosphate carboxylase/oxygenase (EC 4.1.1.39, Rubisco) has been shown to increase in vitro after oxidative treatments that affect cysteine thiols. A limited incubation of oxidized (pretreated with the disulfide cystamine) Rubisco from *Chlamydomonas reinhardtii* with subtilisin or proteinase K generated fragments of molecular mass about 53 kDa (band I in SDS−PAGE) and 47 kDa (band II) derived from the large subunit (55 kDa) of the enzyme. In contrast, proteolysis of the reduced Rubisco (pretreated with the free thiol cysteamine) produced only the 53 kDa band. The same fragmentation pattern was reproduced with Rubiscos from other algae and higher plants, as well as with other chemical modifications of protein cysteines. N-terminal sequencing of the fragments showed that band I arised from clipping the unstructured N-terminal stretch of the large subunit up to Lys18. Band II was generated by a cleavage close to Val69. The increased susceptibility of the oxidized form resulted from proteases gaining access to a loop (from Ser61 to Thr68) located between stretches of secondary structure that form the N-terminal domain. Native electrophoresis and kinetic analysis of fragment accumulation during subtilisin digestion demonstrated that subunit dissociation was induced by the proteolytic processing at the Ser61−Thr68 loop, which is characteristic of the oxidized Rubisco. Holoenzyme dissasembly was readily followed by the full degradation of the released subunits. In contrast, the limited processing to band I observed with the reduced enzyme did not compromise the quaternary structure of the Rubisco hexadecamer, thus preventing further proteolysis.

The CO_2-fixing photosynthetic enzyme ribulose 1,5-bisphosphate carboxylase/oxygenase (EC 4.1.1.39, Rubisco) of photosynthetic eukaryotes is an oligomeric protein composed of eight large subunits (ca 55 kDa) and eight small subunits (ca 15 kDa). The three-dimensional structure of this enzyme has been determined in a number of eukaryotic species including the unicellular green alga *Chlamydomonas reinhardtii* (*1*, *2*). General aspects of the correlation between Rubisco structure and function have been recently reviewed (*3*, *4*). The native hexadecamer accumulates to high concentrations in the chloroplast stroma without apparent turnover during growth and expansion phases. In contrast, the enzyme is usually degraded in a rapid and selective manner during the early stages of natural or stress-induced senescence (*5*). The molecular mechanisms that cause this change of turnover rate are yet to be determined, but the degradative process is known to be preceded in some instances by oxidative modifications that induce Rubisco polymerization (*6*) and association to membranes (*7*). Therefore, it seems plausible that the oxidation of Rubisco may target, in one way or another, the enzyme for degradation. Rubisco subunits are known to undergo several post-translational modifications; the physiological function of many of them remains poorly known (*8*). It has been suggested that reactive oxygen species (ROS), which are readily generated by the photosynthetic apparatus inside the chloroplast under stress or senescence conditions, may modify the Rubisco, facilitating its subsequent degradation by proteases (*9*, *10*). Accordingly, in vitro proteolysis of Rubisco that had been previously exposed to ROS (*10*) produced fragments that were identical in size to those observed in vivo when isolated chloroplasts were incubated with oxygen radical promoters (*9*). Furthermore, it has been argued that ROS may directly cleave the enzyme at specific sites (*11*−*14*). Here again, Rubisco fragments obtained in vitro by means of ROS-generating systems (*11*, *13*) matched the size of those seen in vivo when isolated chloroplasts were illuminated in the presence of inhibitors of oxygen-scavenging enzymes (*12*). Taken together, the results strongly suggest that these mechanisms of degradation mediated by oxygen radicals may indeed operate inside the chloroplast when the defenses against ROS are overridden. In addition, the glycation of Rubisco lysine residues by ascorbic acid has also been recently proposed as a candidate mechanism for regulating Rubisco turnover (*15*). Besides, there have been several reports indicating that the proteolytic susceptibility of the native Rubisco in vitro increases through treatments that produce oxidative modification of cysteine thiols (*6*, *16*−*18*). Because stress processes are known to promote oxidation of Rubisco cysteines in vivo (*7*, *19*−*21*), it has been

† This work was supported by Grants PB1998-1445 and BMC2003-03209 from DGESIC-MCYT and by a fellowship of the Generalitat Valenciana (awarded to J.M.-N.).

* To whom correspondence should be addressed. Phone: 34-963543014. Fax: 34-963544635. E-mail: joaquin.moreno@uv.es.

10.1021/bi035713j CCC: $25.00
Published on Web 11/19/2003

suggested that this mechanism of proteolytic sensitization may also contribute to the selective and extensive degradation of Rubisco that takes place during natural or stress-induced senescence of photosynthetic tissues (*22*). The link between Rubisco cysteine modification and in vivo turnover has been further supported by the report that the enzyme of a *C. reinhardtii* mutant, in which the conserved cysteine 172 of the large subunit has been replaced by serine (i.e., the C172S Rubisco mutant), undergoes delayed degradation in vivo when the cells are subjected to different stresses (*18*). Recently, a similar result was also obtained when the same residue was mutated in a cyanobacterial Rubisco (*23*).

Although there have been several reports on proteolysis of Rubisco by exogenous (*24*, *25*), endogenous (*26*−*32*), or even chloroplastic (*33*−*35*) proteases, their activity has not been tested by comparing the effect on the reduced and oxidized carboxylase, with two exceptions. In one case, Rubisco was previously modified by ROS before being subjected to proteolysis (*10*). However, exposure of proteins to oxygen radicals results in miscellaneous oxidative modifications on different amino acids (*36*). Thus, their effects on Rubisco proteolysis are hardly representative of cysteine thiol oxidation. In another instance, the endogenous proteolytic activity of *Lemna minor* has been assayed against native, oxidized, and oxidatively polymerized Rubisco from the same organism (*37*). Rubisco oxidation was achieved in this case by incubation with an endogenous enzymatic system (Rubisco oxidase) that is known to induce both disulfide and nondisulfide covalent oxidative modifications on Rubisco (*19*, *37*), the latter presumably on residues other than cysteine. Besides, this study analyzed only differences in global proteolytic activity on the diverse substrates, not attempting to examine possible changes in the proteolytic pattern. Therefore, little is currently known at the molecular level about the reasons for the increased proteolytic susceptibility of Rubisco caused specifically by cysteine oxidation. We have studied the proteolysis of Rubisco in the reduced and oxidized states achieved through incubation, respectively, with cysteamine and cystamine, a thiol/disulfide pair that is known to switch the enzyme between the protease-resistant and -sensitive forms (*17*, *18*) by reacting solely with cysteine residues through disulfide exchange (*38*). In this paper we present results that offer some insight into the molecular mechanism by which cysteine oxidation facilitates the proteolysis of Rubisco.

EXPERIMENTAL PROCEDURES

Biological Material and Growth Conditions. Wild-type *C. reinhardtii* strain 2137 mt+ was a gift from Dr. Robert J. Spreitzer (University of Nebraska at Lincoln). For Rubisco extraction, *C. reinhardtii* was grown on acetate-supplemented medium in light as previously described (*18*). *Euglena gracilis* strain Z (Pringsheim) was obtained from the Göttingen Algal Culture Collection (University of Göttingen, Germany) and was grown on Euglena broth (DIFCO, Detroit, MI) at the same light intensity, temperature, and shaking conditions as *C. reinhardtii*. Leaves from spinach (*Spinacia oleracea*), rice (*Oryza sativa*), and mulberry tree (*Morus alba*) were sampled from local cultures.

Rubisco Purification. Rubisco from *C. reinhardtii* and from *E. gracilis* was extracted by sonication and purified by successive steps of ammonium sulfate fractionation, sucrose density gradient centrifugation, and DEAE-cellulose chromatography as previously described (*17*). Rubisco from spinach, rice, and mulberry leaves was extracted in a blade homogenizer with 4 mL/g of fresh weight of extraction buffer (100 mM Tris−H_2SO_4, 10 mM $MgSO_4$, 20 mM 2-mercaptoethanol, pH 8.0). The homogenate was filtered through cheesecloth, and the filtrate was stirred with insoluble polyvinylpolypyrrolidone (20 mg/mL) for 5 min. After centrifugation (35000*g* for 10 min), the supernatant was subjected to ammonium sulfate fractionation, sucrose gradient centrifugation, and DEAE-cellulose chromatography as above. All steps of extraction and purification were carried out either under refrigeration at 4 °C or by keeping the extract in an ice bath.

In all cases the final preparation contained more than 95% Rubisco (as estimated from Coomassie Blue stained SDS−PAGE) and was esentially free of nucleic acids (A_{280}/A_{260} higher than 1.7). Prior to its oxidation or reduction, the purified Rubisco was desalted in a Sephadex G-25 column (PD-10, Amersham-Pharmacia Biotech) equilibrated with activation buffer (100 mM Tris−HCl, 10 mM $MgCl_2$, 10 mM $NaHCO_3$, pH 8.2). The Rubisco concentration in purified preparations was determined assuming an average extinction coefficient ($\epsilon^{1\%}$) of 15.7 at 280 nm (based on data reviewed in ref *5*).

Oxidation/Reduction of Rubisco and Proteolytic Assay. Purified Rubisco at an approximate concentration of 0.2 mg/mL in activation buffer was incubated with 20 mM cystamine (for oxidation) or 40 mM cysteamine (for reduction) for 2 h at 30 °C under a N_2 atmosphere in a vacuum oven. For use with redox-sensitive proteases (trypsin and chymotrypsin), excess cystamine or cysteamine was eliminated by desalting in a Sephadex G-25 column (NAP-10, Amersham-Pharmacia Biotech) equilibrated with activation buffer. Proteolytic assays took place immediately afterward. For subtilisin and proteinase K digestion, 80 μL samples of reduced or oxidized Rubisco solution were mixed with 20 μL of the protease (2.5 μg/mL) in activation buffer. The mixtures were incubated in a water bath at 30 °C for fixed times, and the reaction was stopped by addition of 10 μL of 22 mM phenylmethylsulfonyl fluoride (PMSF) in 2-propanol and transfer to ice for 10 min. Afterward, the samples were prepared for electrophoresis. For SDS−PAGE, 55 μL of 3 × SDS loading buffer [0.188 M Tris−HCl, 0.6 M 2-mercaptoethanol, 6% (w/v) SDS, 30% (v/v) glycerol, 0.075% (w/v) bromophenol blue, pH 6.8] was added, and the mixture was boiled for 5 min. For native PAGGE, 55 μL of 3 × nondenaturing loading buffer [0.2 M Tris−HCl, 0.6 M 2-mercaptoethanol, 25% (v/v) glycerol, 0.075% (w/v) bromophenol blue, pH 8] was mixed in without boiling.

In the case of all other proteases (trypsin, chymotrypsin, and V8-proteinase), the procedure was the same except the proteolytic reaction was stopped directly by adding 50 μL of 3 × SDS loading buffer and immediate boiling. The final concentrations used for each protease are given in the figure captions.

Electrophoresis, Membrane Transfer, and Immunoblotting. Discontinuous SDS−PAGE was performed as previously described (*17*) using either 10% or 14% polyacrylamide in the resolving gel. After electrophoresis, gels were stained with 0.1% (w/v) Coomassie Blue R-250 in 46% (v/v) methanol and 8% (v/v) acetic acid, scanned, and quantified using an image analyzer program (Quantity One, Bio-Rad).

In other instances, proteins were electrotransferred from the gels onto polyvynyldifluoridene (PVDF; Bio-Rad) membranes and immunostained using a rabbit antiserum raised against purified Rubisco from *E. gracilis* as published (*20*). For N-terminal sequencing, the proteins were electrotransferred onto sequencing-grade PVDF membranes (Immobilon P^{SQ}, Millipore) and stained briefly with Coomassie Blue R-250 as above. The selected protein bands were cut out and directly delivered to an automatic protein sequencer.

Electrophoresis of native Rubisco was performed either in nondenaturing polyacrylamide gels (PAGE) or in polyacrylamide gradient gels (PAGGE). Nondenaturing PAGE gels were prepared with a 7% (w/v) polyacrylamide resolving gel and a 4% (w/v) polyacrylamide pregel in 0.375 M Tris−HCl buffer, pH 8.9. Electrophoresis was run overnight at 35 V with 50 mM Tris−glycine, pH 8.3, as electrode buffer.

Native 5−30% polyacrylamide gradient gels were prepared in 0.375 M Tris−HCl buffer, pH 8.9. PAGGE was carried out in 50 mM Tris−glycine buffer, pH 8.3, for 2000 V·h. Gels were stained with Coomassie Blue R-250 as above. Alternatively, for identification of assembled polypeptides, the gels were stained with 1% (w/v) Coomassie Blue R-250 in water, and the Rubisco holoenzyme bands were cut out from the gel. The gel pieces were further cut in halves, mixed in an Eppendorf tube with 30 μL of SDS loading buffer [63 mM Tris−HCl, 0.2 M 2-mercaptoethanol, 2% (w/v) SDS, 10% (v/v) glycerol, 0.025% (w/v) bromophenol blue, pH 6.8], and boiled for 5 min. Afterward, the polypeptides were allowed to diffuse out of the gel for 72 h at room temperature. Then, the mixture was centrifuged (1500*g* for 1 min), and the supernatant was loaded onto the SDS−PAGE gel.

Model Fitting. The differential equation systems (eqs 1−3 and other alternatives considered) were numerically solved by means of the Newton method using an Excel sheet. The unknown variables (kinetic constants) were determined by adjusting the model output to the experimental points by minimizing the sum of square deviations with the Microsoft Excel Solver tool. The goodness of fit was evaluated by the χ^2-test (using a separate estimation of analytical variability through the independent duplication of 26 samples) and by the determination coefficient (*39*). The standard error of the calculated constants was estimated using the jackknife procedure (*40*).

RESULTS

The Proteolytic Fragmentation Pattern of the Large Subunit of Rubisco Depends on the Redox State of Its Cysteines. Purified Rubisco from *C. reinhardtii* was subjected to a thiol-oxidizing (incubation with the disulfide cystamine) or disulfide-reducing (incubation with the free thiol cysteamine) treatment before being exposed to broad-specificity proteases, such as proteinase K and subtilisin. The proteolysis of the oxidized Rubisco generated fragments of molecular mass about 53 kDa (band I in SDS−PAGE) and 47 kDa (band II) derived from the large subunit (55 kDa) of the enzyme, within the first 40 min of assay. In contrast, proteolysis of the reduced enzyme produced during the same period only the 53 kDa fragment (band I) (Figure 1A). A similar fragmentation pattern of oxidized and reduced forms was obtained when proteolysis was carried out with Rubiscos from other species such as *E. gracilis*, spinach (*S. oleracea*), mulberry tree (*M. alba*), and rice (*O. sativa*) (Figure 1B).

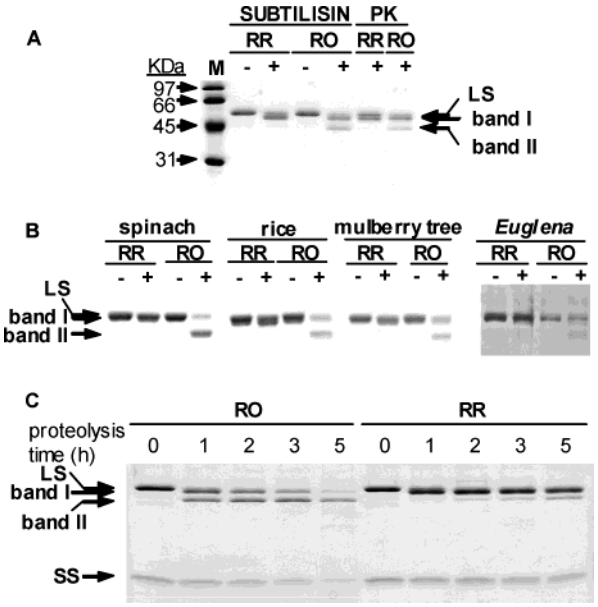

FIGURE 1: Proteolysis of reduced (RR) and oxidized (RO) Rubisco with broad-specificity proteases. The positions of the intact large (LS) and small (SS) subunits of Rubisco, as well as the degradation fragments termed band I and band II, after SDS−PAGE are indicated with arrows. (A) Purified Rubisco (0.1 mg/mL in activation buffer) from *C. reinhardtii* was incubated at 30 °C in the presence (+) or absence (−) of subtilisin or proteinase K (PK) at a final concentration of 0.5 μg/mL. After 40 min, the reaction was stopped and the products were run in SDS−PAGE together with molecular mass markers (M). (B) Purified Rubiscos (0.1 mg/mL in activation buffer) from spinach, rice, mulberry tree, and *E. gracilis* were incubated at 30 °C in the absence (−) or presence (+) of subtilisin at 0.06 μg/mL or 0.1 μg/mL (spinach) for 20 min (*Euglena*), 40 min (rice and mulberry tree), or 50 min (spinach). (C) Purified Rubisco (0.1 mg/mL in activation buffer) from *C. reinhardtii* was incubated at 30 °C for different times (up to 5 h) with subtilisin (0.5 μg/mL).

These species were selected because of their sequence divergence, sharing only a limited number of highly conserved cysteine residues. The fact that all enzymes experienced the same change of proteolytic pattern upon cysteine oxidation suggests that this may be a general response among eukaryotic Rubiscos. In all cases, the electrophoretic bands I and II, corresponding to large subunit fragments generated by proteolysis, were not strictly homogeneus but consisted of overlapping polypeptides of similar size. Nevertheless, this size heterogeneity receded at longer times of proteolysis, converging to a lowest band limit (Figure 1C). This was probably due to repeated clipping ("shaving") of the protease-sensitive domains until a proteolysis-resistant core of fixed size accumulated. The molecular weights ascribed above to the electrophoretic bands always refer to this lowest band limit.

Longer incubations with subtilisin (up to 5 h) evidenced that band II was also produced with the reduced Rubisco but at a much lower rate. Band II was only detected after 1 h, when almost all the large subunit had been previously processed to band I (Figure 1C). The total amount of large subunit seen in the gel (intact subunit plus fragments) decreased steadily in the case of the oxidized enzyme (Figure 1C). In contrast, the total large subunit stain of the reduced Rubisco experienced only a very slight decrease, accumulating mostly as band I. Furthermore, the proteolytic processing of the small subunit (15 kDa) was also much slower in the

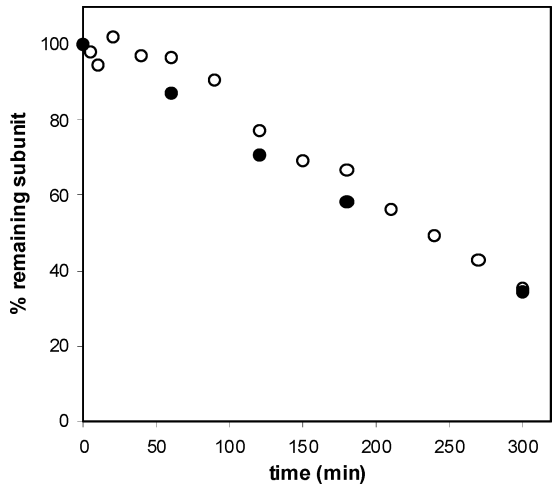

FIGURE 2: Unrestricted degradation of the large (○) and small (●) subunit of *C. reinhardtii* Rubisco by subtilisin. Samples of purified and oxidized Rubisco (0.1 mg/mL in activation buffer) were incubated with subtilisin (0.5 μg/mL). The incubation mixtures were stopped at different times (up to 300 min), and run in SDS−PAGE. The intact Rubisco subunits and the large subunit fragments (band I and band II) were quantified from the Coomassie stained gels. The values obtained for band I and band II were compensated for the loss of mass and added to the value of the intact large subunit. The final values, which reflect the amount of subunit remaining in the gel (i.e., not subjected to unrestricted degradation), are represented as percentages of the initial content.

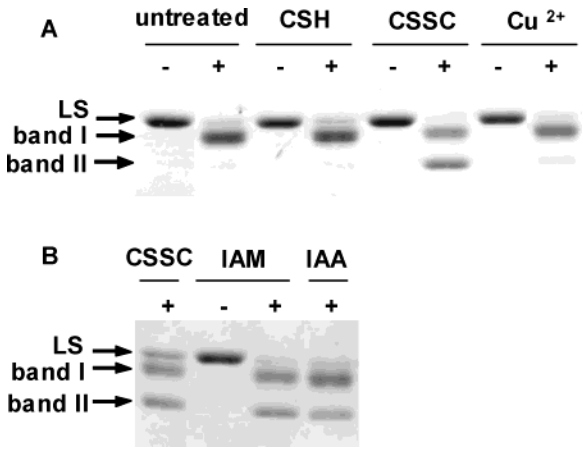

FIGURE 3: Subtilisin proteolysis of Rubisco previously treated with different chemical agents that modify cysteine residues. Treatments were (A) CSH = cysteamine (40 mM final concentration), CSSC = cystamine (20 mM), Cu^{2+} = copper sulfate (25 μM) and (B) CSSC = cystamine (20 mM); IAM = iodoacetamide (20 mM); IAA = iodoacetic acid (20 mM). Samples of purified Rubisco (0.1 mg/mL in activation buffer) were incubated with the indicated agents at 30 °C for 2 h under a nitrogen atmosphere in a vacuum oven. Afterward the mixtures were further incubated with (+) or without (−) subtilisin (final concentration 0.5 μg/mL) in a water bath at 30 °C for 1 h (except CSSC in (B) for 20 min) before SDS−PAGE was run. The positions of the intact large subunit (LS) of Rubisco, as well as the degradation fragments termed band I and band II, after SDS−PAGE are indicated with arrows.

reduced Rubisco than in the oxidized enzyme, although it did not produce detectable fragments in either case (Figure 1C). This suggests that both subunits of the oxidized Rubisco were degraded further to amino acids or oligopeptides too small to be detected as bands in SDS−PAGE. We will term this final step "unrestricted" proteolysis, in opposition to limited proteolysis that gives rise to fragments of relatively high molecular mass and definite size. Unrestricted proteolysis may be monitored through the time course of the sum of the intact subunit and all fragments derived from it, after compensating the Coomassie blue stain intensity for the loss of mass (i.e., multiplying the measured intensity by the mass of the intact subunit and dividing by the mass of the fragment). When this was done for the large and small subunits of the oxidized Rubisco, it became clear that the unrestricted degradation of both subunits took place at the same rate (Figure 2). This parallelism probably reflects the fact that unrestricted proteolysis may be only possible after dismantling of the quaternary structure of Rubisco. Because degradation of the free subunits is expected to be much faster, the rate of unrestricted proteolysis is likely to be limited by holoenzyme disassembly. Since the reduced Rubisco experienced very little unrestricted proteolysis, even after 5 h of incubation (Figure 1C), it appears that subunit dissociation was promoted directly or indirectly by the oxidized state of the enzyme.

The Differential Proteolytic Pattern Can Be Induced by Diverse Modifications of Cysteines. To investigate if the modification of the proteolytic pattern resulted only from the oxidation of cysteines with disulfides, or even more specifically with cystamine, Rubisco was treated with several agents (other than disulfides) that are known to react with cysteine residues, and was subjected afterward to proteolysis with subtilisin. Alkylating reagents such as iodoacetamide or iodoacetic acid induced the characteristic change of proteolytic pattern, producing band II at short incubation times as with cystamine (Figure 3). Because iodoacetamide, iodoacetic acid, and cystamine attach, respectively, a neutral, a negatively charged, and a positively charged group to the modified cysteines, a specific charge effect can be ruled out as a cause of the differential fragmentation. Band II was also generated (though to a lower amount) after cysteine modification by free radical modification (induced by Cu^{2+}) (Figure 3). The lesser accumulation of band II after treatment with Cu^{2+} is likely to reflect the incomplete modification of cysteines, as judged by the partial inactivation of the enzyme achieved under similar conditions (*18*). Taken together, these results demonstrate that the switch of the proteolytic pattern is not the result of a particular derivatization of the cysteines but appears to be caused by the suppression of certain thiol groups that are present in the untreated enzyme.

The Differential Proteolysis of the Oxidized Rubisco Arises Because Proteases Gain Access to a Conserved 8-Amino Acid Loop upon Oxidation of Cysteines. N-terminal sequencing of the limit fragments derived from subtilisin digestion of the *C. reinhardtii* Rubisco showed that band I arised from clipping the large subunit at Lys18 (Figure 4), probably releasing the unstructured N-terminal end, as has been previously reported to occur through trypsin digestion (*24*). Band II was generated by cleavage between Thr68 and Val69 (Figure 4). Since band I and band II match the sizes expected after removal of the N-terminal pieces when cleaved at the determined sequences, an eventual processing at the C-terminus would be restricted to a few residues. Proteolysis of reduced and oxidized Rubisco with residue-specific proteases (trypsin, chymotrypsin, and V8-proteinase) always produced a fragment similar to band I, but only chymotrypsin acting on the oxidized enzyme released a fragment similar to band II (Figure 5). A survey of the potential target sites for these proteases suggested that band I was produced by

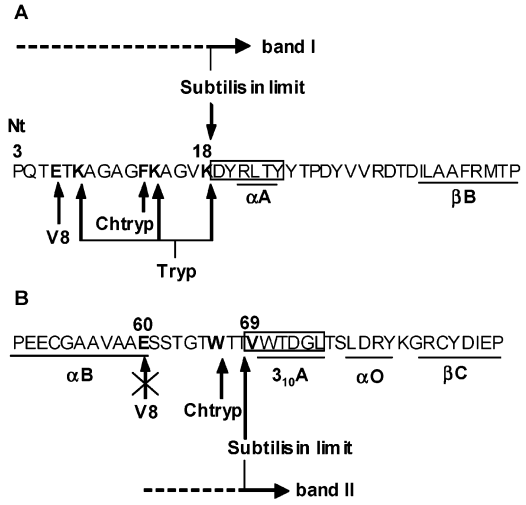

FIGURE 4: Partial sequences of the large subunit of *C. reinhardtii* Rubisco including the N-terminus of band I (A) and band II (B) at their lowest size limit generated by subtilisin. Determined N-terminal sequences are boxed. Secondary structure elements (taken from ref *2*) are underlined. Presumed cleavage sites (according to Figure 4) for trypsin (Tryp), chymotrypsin (Chtryp), V8-proteinase (V8), and subtilisin are indicated by arrows. Deduced protease-sensitive sequence spans for band I and band II are marked by horizontal dotted lines. (A) N-terminal sequence of the mature large subunit (residues 3−44). (B) Sequence around the cleavage site for band II (residues 50−89). The potential cleavage point for V8-proteinase at Glu60 (where no cut was actually observed) is indicated by a canceled arrow.

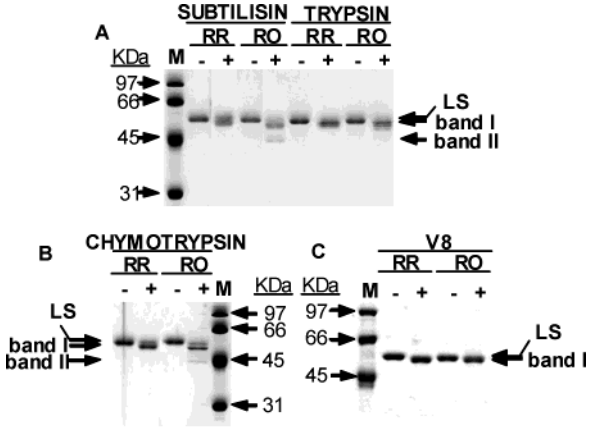

FIGURE 5: Proteolysis of reduced (RR) and oxidized (RO) Rubisco from *C. reinhardtii* with residue-specific proteases: trypsin (A), chymotrypsin (B), and V8-proteinase (C). Proteolysis with subtilisin (A) is included for comparison. Purified Rubisco (0.1 mg/mL in activation buffer) was incubated at 30 °C in the presence (+) or absence (−) of protease at 0.5 or 0.6 μg/mL (V8) for 40 or 140 min (V8). The products of proteolysis were run in SDS−PAGE together with molecular mass markers (M). The positions of the intact large subunit (LS) of Rubisco, as well as the degradation fragments termed band I and band II, are indicated with arrows.

clipping anywhere along the unstructured N-terminal end up to Lys18 (Figure 4). On the other hand, band II resulted from proteases reaching a loop of 8-amino acids (from Ser61 to Thr68) located between stretches of secondary structure that form the N-terminal domain (*1*, *2*) (Figure 4). The accesibility of the proteases to this loop was delimited by an α-helix element ending in Glu60 (at which the V8-proteinase seemed unable to cut) and the Val69, which was the N-terminal residue of band II at the lowest mass limit achieved by subtilisin. The sequence of the Ser61−Thr68 loop (which

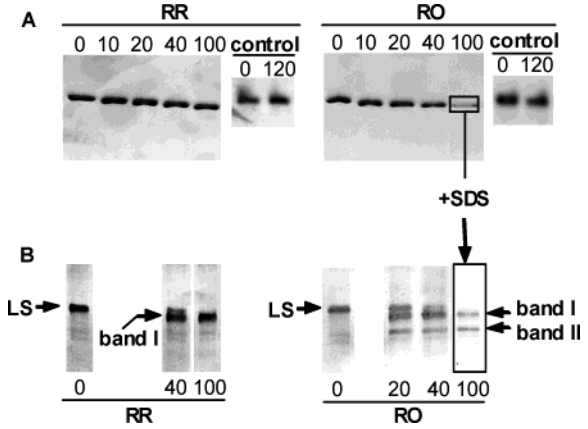

FIGURE 6: Time course of proteolysis of reduced (RR) and oxidized (RO) Rubisco from *C. reinhardtii* with subtilisin as monitored by PAGGE (A) or by SDS−PAGE of the polypeptides recovered from the holoenzyme band obtained in PAGGE (B). Purified Rubisco (0.1 mg/mL in activation buffer) was incubated at 30 °C with subtilisin (0.5 μg/mL). Samples of the incubation mixture were taken at different times, stopped, and run in PAGGE. The Rubisco holoenzyme bands were cut out, and the polypeptides were allowed to diffuse in SDS loading buffer. Afterward, the extracts were reloaded onto the SDS−PAGE gel and immunoblotted. The numbers on the top (A) or bottom (B) of the lanes represent the time of proteolysis in minutes. Controls in (A) correspond to Rubisco incubated in the same conditions without subtilisin and run in 7% PAGE.

does not contain cysteines) is highly conserved among eukaryotic Rubiscos. Results suggest that oxidation of cysteines favors a wider exposure of this loop to proteolytic attack.

The Differential Proteolysis of the Oxidized Rubisco Induces Holoenzyme Disassembly. Native electrophoresis in polyacrylamide gradient gels of subtilisin-digested Rubisco revealed a limited decrease of the holoenzyme size associated with proteolysis (Figure 6). The lowest size limit was the same with the reduced and the oxidized Rubisco. From the estimated molecular weight loss of the proteolytically processed holoenzyme, it may be inferred that the small N-terminal piece (up to Lys18) was released from the holoenzyme core after proteolysis in both the reduced and oxidized forms, while the bigger fragment (up to the Ser61−Thr68 loop, resulting from the cut that originates band II) remained attached to the hexadecamer until its final unrestricted degradation. In fact, recovering the oxidized holoenzyme after 100 min of proteolysis from the PAGGE bands and rerunning the sample in SDS−PAGE demonstrated that large subunits processed to band II were indeed integrated in the quaternary structure (Figure 6). The complementary piece (from the processed N-terminus up to somewhere in the Ser61−Thr68 loop) was probably too small (less than 8 kDa) to be detected as a band in SDS−PAGE. Once again, it became clear that the band of the oxidized Rubisco experienced a significant intensity decrease throughout the proteolytic process while the reduced holoenzyme remained almost unaffected (Figure 6). As discussed above, unrestricted proteolysis is expected to take place only after holoenzyme disassembly. Because the oxidized Rubisco does not disassemble at 30 °C during the assay period if not subjected to proteolysis (see the control lane in Figure 6), it follows that subunit dissociation must be promoted by the proteolytic cuts. Furthermore, the fact that the reduced Rubisco does not disassemble either after massive processing

to band I (e.g., after 100 min of proteolysis) (Figure 6) suggests that holoenzyme dismantling may be specifically induced by the cleavage at the Ser61−Thr68 loop, which is characteristic of the oxidized Rubisco.

Kinetic Analysis Confirms That Unrestricted Proteolysis of Rubisco Depends on Previous Processing to Band II. To further explore Rubisco proteolysis, we measured the amount of intact large subunit (*z*) as well as those of the detectable subproducts, the 53 kDa band I (p_1) and 47 kDa band II (p_2) fragments, throughout the time course of Rubisco degradation by subtilisin and attempted to adjust the results to a quantitative kinetic model. With this we sought to reassess the conclusions drawn hitherto, integrating them into a minimum set of mathematical premises that may capture the essential features of the proteolytic process by fitting the experimental data without drift.

Because of the relatively low concentration of the specific bonds to be hydrolyzed, we assumed (as usually done) that each proteolytic cut done on Rubisco should follow first-order kinetics. Under these conditions (substrate concentration much lower than the Michaelis constant), the competitive inhibition between the different proteolytic substrates would be negligible and need not be considered. The apparent first-order constants would be obviously dependent on the particular protease concentration used in the assay. We defined k_1 as the first-order constant for the cleavage at the N-terminus (producing band I) acting only on intact large subunits (i.e., on *z*). The 47 kDa fragment (band II in SDS−PAGE), resulting from the cut at the Ser61−Thr68 loop, may arise directly from cleaving the intact large subunit, or from further processing of band I. Prospective fitting of alternative models to the data suggested that band II was indeed generated either way. We allowed different rate constants for the direct processing of the intact large subunit (k_2 acting on *z*) and for degradation of band I (k_2' acting on p_1). Furthermore, Rubisco also underwent unrestricted degradation, probably as a result of holoenzyme disassembly favored by the previous processing of some of the subunits to band II. This final degradation step would eliminate both intact (*z*) and processed (p_1 and p_2) large subunits (since they may integrate together the holoenzyme molecules to be disassembled) but at a rate that would be dependent on the relative p_2. Therefore, we assumed that unrestricted degradation was also first-order with a limit rate constant (k_3) modulated by a factor (θ, taking values between 0 and 1) that would be an undetermined but monotonically increasing function of *f*, the current average fraction of subunits processed to band II [i.e., $f = p_2/(z + p_1 + p_2)$]. All the above may be schematically represented (Scheme 1) and summmarized in the following equations:

$$dz/dt = -(k_1 + k_2 + \theta k_3)z \quad (1)$$

$$dp_1/dt = k_1 z - (k_2' + \theta k_3)p_1 \quad (2)$$

and

$$dp_2/dt = k_2 z + k_2' p_1 - \theta k_3 p_2 \quad (3)$$

We tried different functions of *f* for factor θ. Although the simple identity $\theta = f$ gave already a reasonable adjustment to the experimental points, a distinctly better fitting was obtained with $\theta = f^2$. Because the probability of having any given pair of large subunits both cut at the Ser61−Thr68 loop should be proportional to f^2, we interpreted this result as that disassembly might be dependent on the cleavage of both large subunits of any of the four dimers that integrate the holoenzyme core. Tentatively, we also allowed for protease inactivation (e.g., by self-digestion), letting the first-order constants decay with time according to auxiliary equations. However, this supplementary assumption did not significantly improve the fitting, always giving very low values for the decay rates. Thus, for simplicity, the protease activity was assumed to remain stable.

Scheme 1: Schematic Representation of the Proteolytic Processing of the Rubisco Large Subunit by Subtilisin[a]

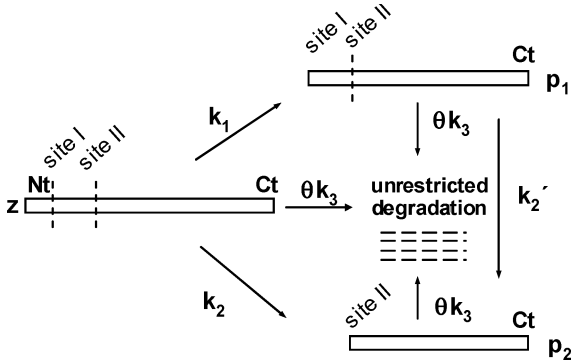

[a] According to the kinetic model described by eqs 1−3. Arrows (with associated kinetic constants) indicate the postulated transformations among the intact subunit (*z*), the band I (p_1) and band II (p_2) fragments, and the small peptides and amino acids that result from unrestricted degradation. Nt and Ct label the N-terminal and C-terminal end of the large subunit. Sites I and II are the processing sites for generation of band I and band II, respectively.

The system of differential equations (eqs 1−3 with $\theta = f^2$) was numerically solved by adjusting the values of the unknown rate constants by minimizing the sum of square deviations from the experimental points. The model gave a remarkable adjustment, free of obvious systematic deviations for both the reduced and oxidized Rubisco (Figure 7), with an overall coefficient of determination higher than 0.99 [i.e., the model explained more than 99% of the observed change (*39*)], and a divergence from predicted values fully compatible with experimental error (χ^2 of 17.2 and 23.2 with 38 degrees of freedom, respectively, for the reduced and oxidized Rubisco). The introduction of alternative hypotheses, such as strictly sequential cuts, a single rate constant for generation of band II, or suppression of factor θ, produced worse fittings with systematic departure of the experimental points from the predicted curve in all cases (not shown). The estimated values of the constants for the reduced and oxidized Rubisco are listed in Table 1. The values of k_1 for the reduced and oxidized enzyme were similar, suggesting that the redox state does not have a substantial effect on the susceptibility to the N-terminal cut. In contrast, the values of k_2' and k_2 were clearly higher for the oxidized Rubisco, as expected from the differential proteolytic pattern shown in Figure 1. The fact that k_2 was significantly higher than k_2' in both redox states indicates that the previous clipping of the N-terminal end imposes a restriction to the subsequent cut at the Ser61−Thr68 loop. The limit constant k_3 represents the rate of unrestricted proteolysis that would be observed if all large subunits were previously cut at the Ser61−Thr68 loop. Because subunit digestion may take place rapidly and

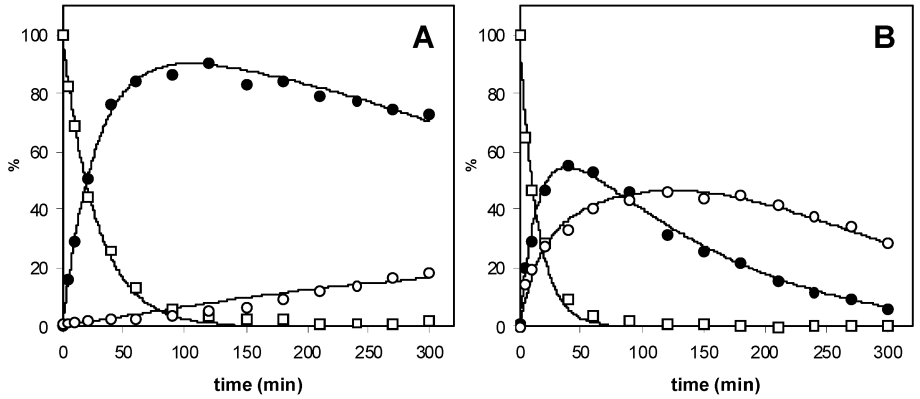

FIGURE 7: Time course of the intact large subunit (□), band I (●), and band II (○) during proteolysis of reduced (A) and oxidized (B) Rubisco from *C. reinhardtii* with subtilisin. Samples of purified Rubisco (0.1 mg/mL in activation buffer) were incubated with subtilisin (0.5 μg/mL). The incubation mixtures were stopped at different times (up to 300 min), and run in SDS−PAGE. The intact Rubisco subunits and the large subunit fragments (band I and band II) were quantified from the Coomassie stained gels. The values obtained for band I and band II were normalized to the whole large subunit by compensating for the loss of mass. All values are represented as percentages of the initial content of the intact large subunit. The curves fitting the experimental points were obtained from the model described by eqs 1−3 after the values of the unknown rate constants were adjusted by minimizing the sum of square deviations.

Table 1: Estimated Values for the First-Order Rate Constants of the Kinetic Model[a]

kinetic constant	reduced Rubisco	oxidized Rubisco	kinetic constant	reduced Rubisco	oxidized Rubisco
k_1	0.0358 ± 0.0014	0.047 ± 0.004	k_2'	0.00072 ± 0.00012	0.0044 ± 0.0003
k_2	0.0008 ± 0.0006	0.022 ± 0.003	k_3	0.029 ± 0.014	0.0092 ± 0.0003

[a] Constants were calculated by adjusting the model to the experimental points by minimization of the sum of square deviations. Values ± standard error are given in inverse minutes.

efficiently after dissociation from the holoenzyme, it is likely that k_3 does in fact measure the disassembly rate-limiting step. Although k_3 could not be determined with high precission for the reduced Rubisco (due to the low unrestricted degradation in the reduced state), it does not appear to be smaller than the value for the oxidized enzyme (Table 1). This suggests that the redox state of Rubisco does not directly affect the rate of holoenzyme dismantling at physiological temperatures. Therefore, it might be concluded that the step that is actually critical for redox regulation of disassembly (and subsequent unrestricted proteolysis) is the cleavage at the Ser61−Thr68 loop.

DISCUSSION

The selective oxidation of cysteine residues of Rubisco is known to increase the sensitivity of the enzyme to proteases (*17*, *18*). It seems likely that this shift results from subtle structural modifications promoted by cysteine oxidation. Since all Rubisco structures elucidated to date correspond to reduced enzymes, the presumed conformational changes produced by oxidation are yet to be determined. In the present work we have used broad specificity proteases as structural probes to explore conformational changes induced by cysteine oxidation and to identify target sequences for Rubisco degradation, which may be potentially used in vivo too. In addition, we have examined the consequences of proteolytic cleavage at specific sites for holoenzyme disassembly and full degradation of the subunits. All these effects have been integrated into a mathematical model that fits the experimental data satisfactorily, providing quantitative values for the rate constants of the different steps.

We have shown that the main effects of cysteine oxidation on the proteolytic susceptibility of Rubisco are a much faster processing of the large subunit at a specific site (the Ser61−Thr68 loop, which becomes exposed upon oxidation) and a concomitant increase in the rate of unrestricted proteolysis. These effects are robust in the sense that they do not appear to depend on the particular oxidative modification (Figure 3). Besides, the fact that the same redox-regulated proteolytic pattern has been observed with sequence-diverging Rubiscos from different species (Figure 1) suggests that this is a conserved feature that may have a physiological value. Moreover, the critical redox-sensor residues that operate the oxidative switch are likely to be among the highly conserved cysteines that are common to the Rubiscos of these species. These are the cysteines 84, 172, 192, 247, 284, 427, and 459 of the large subunit and cysteine 83 of the small subunit (*C. reinhardtii* numbering). In fact, the site-directed substitution of one of these cysteines (Cys 172 of the large subunit) by a redox-insensitive residue has already been shown to alter the proteolytic susceptibility of the Rubisco in vitro and in vivo (*18*, *23*).

We have identified two sites in the Rubisco large subunit structure that are sensitive to hydrolysis by broad-specificity proteases. The first one, at the unstructured N-terminal stretch (up to Lys 18), was already known through previous studies of Rubisco proteolysis carried out with trypsin (*24*). Our results indicate that this site is unresponsive to the redox state of the Rubisco cysteines. In contrast, the sensitivity of the second site, at the conserved loop between residues 61 and 68, is highly dependent on the oxidation of cysteine residues, the relevant rate constants being 27-fold (k_2) or 6-fold (k_2') higher for the oxidized enzyme (Table 1). The proteolytic accesibility of this second site is also dependent on the contingency of a previous processing at the first site. The difference between the values of k_2 and k_2' (Table 1) indicates that the removal of the unstructured N-terminal stretch somehow causes a change of conformation on the remaining large subunit that makes further processing at the Ser61−Thr68 loop difficult. This was not totally unexpected

since it has already been reported that this single N-terminal cleavage does in fact inactivate the enzyme (*24*). Thus, the structural and functional effects of the N-terminus elimination should reach at least as far as the catalytic site. Nevertheless, the physiological significance of this redox-independent clipping of the N-terminus is uncertain because in vivo Rubisco may be protected from it by substrate occupation of the catalytic site (*41*−*43*), binding of natural inhibitors (*44*), and postranslational modifications (in particular, the trimethylation of Lys14 observed in some species) (*25*). In any case, the N-terminal processing cannot trigger the full degradation of Rubisco, generating instead a resistant core not prone to further proteolysis as observed with the reduced enzyme. In contrast, the processing at the Ser61−Thr68 loop induces the dismantling of the holoenzyme and, thereby, the full proteolysis of the released subunits. It has been recently suggested that the oxidation of cysteine residues may itself promote subunit dissociation (*23*). However, this assertion was based on experiments in which cysteine oxidation was achieved using 5,5′-dithiobis(2-nitrobenzoate) (DTNB). It is likely that the dissociation of subunits results in this case from the steric constraints imposed by the mixed disulfides of the cysteines with the bulky thionitrobenzoate moiety. In fact, it has been known for a long time that derivatizing the Rubisco cysteines with benzoates (e.g., reaction with *p*-chloromercuribenzoate) breaks the holoenzyme into subunits (*45*). Nevertheless, our results show clearly that the quaternary structure is not lost, even after prolonged incubation at 30 °C (control in Figure 6), when oxidation is performed with a small disulfide such as cystamine. It appears that subunit dissociation (a requisite and a limiting step for unrestricted degradation of Rubisco) rather results from the redox-sensitive proteolytic processing at the Ser61−Thr68 loop. In our kinetic model, the limit constant for disassembly (k_3) is modulated at any time by factor θ, representing the square of the fraction of large subunits processed at the Ser61−Thr68 loop (*f*). The divergence of the experimental points from the predicted curve when this factor is dropped indicates that disassembly and unrestricted degradation of Rubisco depend indeed on a previous cut at this site. On the other hand, the quadratic dependence of θ on *f* suggests that the process is triggered by the cleavage of a given pair of large subunits. It seems plausible that these two subunits should be those that integrate any of the four dimers assembled into the holoenzyme core in equivalent positions. This conjecture is also supported by the structural localization of the Ser61−Thr68 loops at the interface between the two large subunits that integrate the core dimers (*1*, *2*). Our results indicate that the fragments generated by cleavage at the Ser61−Thr68 loop stay attached to the holoenzyme core until its disassembly (Figure 6). The final dismantling of the quaternary structure may result perhaps from the spontaneous detachment of one or several of the pieces.

Oxidative modification is a common physiological mechanism for activating protein turnover (*46*). The proteolytic susceptibilization of Rubisco through cysteine oxidation has been repeatedly mentioned as a plausible trigger for the degradation of the enzyme during senescence or stress processes in vivo (*6*, *7*, *16*, *18*, *20*). This work discloses the molecular details of this redox-regulated mechanism, which were unknown hitherto. According to our results, cysteine oxidation favors a specific proteolytic cut at the Ser61−Thr68 loop of the large subunit. In its turn, the repeated cleavage at this site within the same Rubisco molecule (perhaps within the same large subunit homodimer) promotes holoenzyme disassembly and full degradation of the released subunits. Although the involvement of such a mechanism in vivo may prove difficult to establish conclusively, there is compelling indirect evidence that indicates that this process of proteolytic sensitization through cysteine oxidation could be physiologically active. First, the objective existence of redox conditions that oxidize cysteine residues from Rubisco during aging or stress has been demonstrated in several instances (*7*, *19*, *20*). Second, the site-directed substitution of a single conserved cysteine (Cys172) has been shown to delay Rubisco turnover in vivo in both *C. reinhardtii* (*18*) and *Synechocystis* (*23*) mutants under different stress conditions. Therefore, at least this cysteine residue must play a role in the physiological regulation of Rubisco turnover. Third, the incubation of Rubisco with lysates from senescing bean leaves has been shown to generate a large subunit fragment produced by N-terminal cleavage between Thr68 and Val69 (i.e., a piece homologous to band II) as a final product (*47*). This evidences that senescent tissues possess the endogenous machinery that is needed to process the Rubisco specifically at the Ser61−Thr68 loop. In conclusion, while there might exist different alternative proteolytic pathways for Rubisco degradation, the available evidence supports the view that the breakdown of Rubisco triggered by cysteine oxidation and mediated by cleavage at the Ser61−Thr68 loop may represent a significant contribution to in vivo turnover during natural or stress-induced senescence processes.

ACKNOWLEDGMENT

We thank Dr. Pablo J. Miguel (Department of Chemical Engineering, University of Valencia) for providing a program for fitting the experimental data to the kinetic models and for mathematical advice. We also thank Dr. Robert J. Spreitzer (Department of Biochemistry, University of Nebraska at Lincoln) for reviewing the manuscript and for support and Drs.Gautam Sarath (Department of Biochemistry, University of Nebraska at Lincoln) and Juan A. López (Centro Nacional de Biotecnología, Universidad Autónoma de Madrid) for technical advice on protein sequencing.

SUPPORTING INFORMATION AVAILABLE

A figure of the three-dimensional structure of *C. reinhardtii* Rubisco illustrating the relative positions of the unstructured N-terminus, the Ser61−Thr68 loop, and the neighboring cysteine residues. This material is available free of charge via the Internet at http://pubs.aos.org.

REFERENCES

1. Taylor, T. C., Backlund, A., Bjorhall, K., Spreitzer, R. J., and Andersson, I. (2001) First crystal structure of Rubisco from a green alga, Chlamydomonas reinhardtii, *J. Biol. Chem. 276*, 48159−48164.
2. Mizohata, E., Matsumura, H., Okano, Y., Kumei, M., Takuma, H., Onodera, J., Kato, K., Shibata, N., Inoue, T., Yokota, A., and Kai, Y. (2002) Crystal structure of activated ribulose-1,5-bisphosphate carboxylase/oxygenase from green alga Chlamydomonas reinhardtii complexed with 2-carboxyarabinitol-1,5-bisphosphate, *J. Mol. Biol. 316*, 679−691.
3. Spreitzer, R. J., and Salvucci, M. E. (2002) Rubisco: structure, regulatory interactions, and possibilities for a better enzyme, *Annu. Rev. Plant Biol. 53*, 449−475.

4. Andersson, I., and Taylor, T. C. (2003) Structural framework for catalysis and regulation in ribulose-1,5-bisphosphate carboxylase/oxygenase, *Arch. Biochem. Biophys. 414*, 130−140.
5. Ferreira, R. B., Esquivel, M. G., and Teixeira, A. R. (2000) Catabolism of ribulose bisphosphate carboxylase from higher plants, *Curr. Top. Phytochem. 3*, 129−165.
6. Ferreira, R. B., and Shaw, N. M. (1989) Effect of osmotic stress on protein turnover in *Lemna minor* fronds, *Planta 179*, 456−465.
7. Mehta, R. A., Fawcett, T. W., Porath, D., and Mattoo, A. K. (1992) Oxidative stress causes rapid membrane translocation and in vivo degradation of ribulose-1,5-bisphosphate carboxylase/oxygenase, *J. Biol. Chem. 267*, 2810−2816.
8. Houtz, R. L., and Portis, A. R. (2003) The life of ribulose 1,5-bisphosphate carboxylase/oxygenase-posttranslational facts and mysteries, *Arch. Biochem. Biophys. 414*, 150−158.
9. Desimone, M., Henke, A., and Wagner, E. (1996) Oxidative Stress Induces Partial Degradation of the Large Subunit of Ribulose-1,5-Bisphosphate Carboxylase/Oxygenase in Isolated Chloroplasts of Barley, *Plant Physiol. 111*, 789−796.
10. Desimone, M., Wagner, E., and Johanningmeier, U. (1998) Degradation of active-oxygen-modified ribulose-1,5-bisphosphate carboxylase/oxygenase by chloroplastic proteases requires ATP-hydrolysis, *Planta 205*, 459−466.
11. Ishida, H., Nishimori, Y., Sugisawa, M., Makino, A., and Mae, T. (1997) The large subunit of ribulose-1,5-bisphosphate carboxylase/oxygenase is fragmented into 37-kDa and 16-kDa polypeptides by active oxygen in the lysates of chloroplasts from primary leaves of wheat, *Plant Cell Physiol. 38*, 471−479.
12. Ishida, H., Shimizu, S., Makino, A., and Mae, T. (1998) Light-dependent fragmentation of the large subunit of ribulose-1,5-bisphosphate carboxylase/oxygenase in chloroplasts isolated from wheat leaves, *Planta 204*, 305−309.
13. Ishida, H., Makino, A., and Mae, T. (1999) Fragmentation of the large subunit of ribulose-1,5-bisphosphate carboxylase by reactive oxygen species occurs near Gly-329, *J. Biol. Chem. 274*, 5222−5226.
14. Luo, S., Ishida, H., Makino, A., and Mae, T. (2002) Fe2+-catalyzed site-specific cleavage of the large subunit of ribulose 1,5-bisphosphate carboxylase close to the active site, *J. Biol. Chem. 277*, 12382−12387.
15. Yamauchi, Y., Ejiri, Y., and Tanaka, K. (2002) Glycation by ascorbic acid causes loss of activity of ribulose-1,5-bisphosphate carboxylase/oxygenase and its increased susceptibility to proteases, *Plant Cell Physiol. 43*, 1334−1341.
16. Penarrubia, L., and Moreno, J. (1990) Increased susceptibility of ribulose-1,5-bisphosphate carboxylase/oxygenase to proteolytic degradation caused by oxidative treatments, *Arch. Biochem. Biophys. 281*, 319−323.
17. Garcia-Ferris, C., and Moreno, J. (1993) Redox regulation of enzymatic activity and proteolytic susceptibility of ribulose-1,5-bisphosphate carboxylase/oxygenase from *Euglena gracilis*, *Photosynth. Res. 35*, 55−66.
18. Moreno, J., and Spreitzer, R. J. (1999) C172S substitution in the chloroplast-encoded large subunit affects stability and stress-induced turnover of ribulose-1,5-bisphosphate carboxylase/oxygenase, *J. Biol. Chem. 274*, 26789−26793.
19. Ferreira, R. B., and Davies, D. D. (1989) Conversion of ribulose-1,5-bisphosphate carboxylase to an acidic and catalytically inactive form by extracts of osmotically stressed *Lemna minor* fronds, *Planta 179*, 448−455.
20. Garcia-Ferris, C., and Moreno, J. (1994) Oxidative modification and breakdown of ribulose-1,5-bisphosphate carboxylase/oxygenase induced in Euglena gracilis by nitrogen starvation, *Planta 193*, 208−215.
21. Eckardt, N. A., and Pell, E. J. (1995) Oxidative modification of Rubisco from potato foliage in response to ozone, *Plant Physiol. Biochem. 33*, 273−282.
22. Moreno, J., Penarrubia, L., and Garcia-Ferris, C. (1995) The mechanism of redox regulation of ribulose-1,5-bisphosphate carboxylase/oxygenase turnover. A hypothesis, *Plant Physiol. Biochem. 33*, 121−127.
23. Marcus, Y., Altman-Gueta, H., Finkler, A., and Gurevitz, M. (2003) Dual role of cysteine 172 in redox regulation of ribulose 1,5-bisphosphate carboxylase/oxygenase activity and degradation, *J. Bacteriol. 185*, 1509−1517.
24. Gutteridge, S., Millard, B. N., and Parry, M. A. (1986) Inactivation of ribulose-bisphosphate carboxylase by limited proteolysis, *FEBS 196*, 263−268.
25. Houtz, R. L., Stults, J. T., Mulligan, R. M., and Tolbert, N. E. (1989) Post-translational modifications in the large subunit of ribulose bisphosphate carboxylase/oxygenase, *Proc. Natl. Acad. Sci. U.S.A. 86*, 1855−1859.
26. Peoples, M. B., and Dalling, M. J. (1978) Degradation of ribulose-1,5-bisphosphate carboxylase by proteolytic enzymes from crude extracts of wheat leaves. *Planta 138*, 153−160.
27. Peoples, M. B., Frith, G. J. T., and Dalling, M. J. (1979) Proteolytic enzymes in green wheat leaves IV. Degradation of ribulose 1,5-bisphosphate carboxylase by acid proteinases isolated on DEAE-cellulose, *Plant Cell Physiol. 20*, 253−258.
28. Ragster, L., and Chrispeels, M. (1981) Autodigestion in crude extracts of soybean leaves and isolated chloroplasts as a measure of proteolytic activity, *Plant Physiol. 67*, 104−109.
29. Miller, B. L., and Huffaker, R. C. (1982) Hydrolysis of ribulose-1,5-bisphosphate carboxylase by endoproteinases from senescing barley leaves, *Plant Physiol. 69*, 58−62.
30. Thayer, S. S., and Huffaker, R. C. (1984) Vacuolar localization of endoproteianses EP1 and EP2 in barley mesophyll cells, *Plant Physiol. 75*, 70−73.
31. Shurtz-Swirski, R., and Gepstein, S. (1985) Proteolysis of endogenous substrates in senescing oat leaves, *Plant Physiol. 78*, 121−125.
32. Bhalla, P. L., and Dalling, M. J. (1986) Endopeptidase and carboxypeptidase enzymes of vacuoles prepared from mesophylls protoplasts of the primary leaf of wheat seedlings, *J. Plant Physiol. 122*, 289−302.
33. Bushnell, T. P., Bushnell, D., and Jagendorf, A. T. (1993) A Purified Zinc Protease of Pea Chloroplasts, EP1, Degrades the Large Subunit of Ribulose-1,5-Bisphosphate Carboxylase/Oxygenase, *Plant Physiol. 103*, 585−591.
34. Otto, S., and Feierabend, J. (1994) Assay and comparative characterization of the proteolytic degradation of isolated small subunit and holoenzyme of ribulose-1,5-bisphosphate carboxylase/oxygenase in chloroplasts from rye leaves, *J. Plant Physiol. 144*, 26−33.
35. Invernizzi, C., Imhof, J., Burkard, G., Schmid, K., and Boschetti, A. (2002) Effects of mutations at the two processing sites of the precursor for the small subunit of ribulose-bisphosphate carboxylase in Chlamydomonas reinhardtii, *Biochem. J. 366*, 989−998.
36. Halliwell, B., and Gutteridge, J. M. C. (1989) *Free radicals in biology and medicine*, Oxford University Press, Oxford.
37. Albuquerque, J. A., Esquivel, M. G., Teixeira, A. R., and Ferreira, R. B. (2001) The catabolism of ribulose bisphosphate carboxylase from higher plants. A hypothesis, *Plant Sci. 161*, 55−65.
38. Torchinsky, Y. M. (1981) *Sulfur in proteins*, Pergamon Press, Oxford.
39. Chatfield, C. (1983) *Statistics for technology*, Chapman and Hall, London.
40. Efron, B. (1982) *The jackknife, the bootstrap and other resampling plans*, SIAM, Philadelphia.
41. Houtz, R. L., and Mulligan, R. M. (1991) Protection of tryptic-sensitive sites in the large subunit of ribulosebisphosphate carboxylase/oxygenase by catalysis, *Plant Physiol. 96*, 335−339.
42. Chen, Z., and Spreitzer, R. J. (1991) Proteolysis and transition-state-analogue binding of mutant forms of ribulose-1,5-bisphosphate carboxylase/oxygenase from *Chlamydomonas reinhardtii*, *Planta 183*, 597−603.
43. Mulligan, R. M., Houtz, R. L., and Tolbert, N. E. (1988) Reaction-intermediate analogue binding by ribulose bisphosphate carboxylase/oxygenase causes specific changes in proteolytic sensitivity: the amino-terminal residue of the large subunit is acetylated proline, *Proc. Natl. Acad. Sci. U.S.A. 85*, 1513−1517.
44. Khan, S., Andralojc, P. J., Lea, P. J., and Parry, M. A. (1999) 2′-carboxy-D-arabitinol 1-phosphate protects ribulose 1, 5-bisphosphate carboxylase/oxygenase against proteolytic breakdown, *Eur. J. Biochem. 266*, 840−847.
45. Sugiyama, T., Nakayama, N., Ogawa, M., Akazawa, T., and Oda, T. (1968) Structure and function of chloroplast proteins. II. Effect of *p*-chloromercuribenzoate treatment of the ribulose 1,5-diphosphate carboxylase activity of spinach leaf fraction I protein, *Arch. Biochem. Biophys. 125*, 98−106.
46. Stadtman, E. R. (1990) Covalent modification reactions are marking steps in protein turnover, *Biochemistry 29*, 6323−6331.
47. Yoshida, T., and Minamikawa, T. (1996) Successive amino-terminal proteolysis of the large subunit of ribulose 1,5-biphosphate carboxylase/ oxygenase by vacuolar enzymes from French bean leaves, *Eur. J. Biochem. 238*, 317−324.

BI035713J